Cardiac left atrium CT image segmentation for ablation guidance

CARDIAC LEFT ATRIUM CT IMAGE SEGMENTATION FOR ABLATION GUIDANCE

M.M.J. Koppert[1], *P.M.J. Rongen*[2], *M. Prokop*[3], *B.M. ter Haar Romeny*[1], *H.C. van Assen*[1]

[1] Dept. of Biomedical Engineering, Eindhoven University of Technology, Netherlands
[2] Philips Healthcare, Best, Netherlands
[3] Dept. of Radiology, University Medical Center Utrecht, Netherlands

ABSTRACT

Catheter ablation is an increasingly important curative procedure for atrial fibrillation. Knowledge of the local wall thickness is essential to determine the proper ablation energy. This paper presents the first semi-automatic atrial wall thickness measurement method for ablation guidance. It includes both endocardial and epicardial atrial wall segmentation on CT image data. Segmentation is based on active contours, Otsu's multiple threshold method and hysteresis thresholding.

Segmentation results were compared to contours manually drawn by two experts, using repeated measures analysis of variance. The root mean square differences between the semi-automatic and the manually drawn contours were comparable to intra-observer variation (endocardium: $p = 0.23$, epicardium: $p = 0.18$). Mean wall thickness difference is significant between one of the experts on one side, and the presented method and the other expert on the other side ($p < 0.001$). Wall thicknesses found were in the range of 0.5-5.5mm, corresponding to values presented in literature.

Index Terms— Medical Image Analysis, Segmentation, Cardiac Left Atrium, CT, Catheter Ablation

1. INTRODUCTION

The last decade has shown an increasing number of ablation procedures based on anatomic considerations. The largest part concerns catheter ablation of Atrial Fibrillation (AF). During ablation interventions, image guidance is mostly obtained from fluoroscopic imagery, which renders navigation difficult. Alternative methods have to be investigated.

Left atrium (LA) myocardial wall thickness varies over the atrium, and is estimated to be up to 7.7 mm [1]. Lemola et al. [2] found that in 98% of patients in their study a layer of fat between the LA wall and the esophagus was present, although discontinuous in 96%. They suggested a preablation CT scan may be useful. To obtain information about local left atrium (LA) myocardial wall thickness, for selection of ablation duration and energy, requires a presegmentation including both endocardial and epicardial surfaces.

We present a method for *double segmentation* of the LA wall in CT data. CT data both have sufficient image resolution and show the epicardial atrial border at multiple locations [2].

This paper is structured as follows. In Section 2 literature on LA segmentation is discussed; Section 3 elaborates on our method based on active contours. Section 4 presents semi-automatic segmentation results and a comparison to expert drawn contours. Finally, in Section 5 results are discussed.

2. BACKGROUND

Most research on LA segmentation only includes the endocardium, the atrial appendage, and the pulmonary trunks. John and Rahn [3] only segment the endocardium using manual seed points and thresholding, followed by manual object removal and separation at blood pool narrowings. Karim et al. [4] present a number of improvements with respect to [3], only applied to MRA images. Lötjönen et al. [5] built a statistical model from MR images. Their model includes the *epicardial* boundaries of the LA, but in the final segmentation results, only the LA endocardium is presented. Lorenz and Von Berg [6] describe segmentation of the LA blood pool and of the pulmonary veins (PVs) in multislice CT (MSCT) images. They use an active contour-based approach [7] for the LA body and the pulmonary trunks. The model is matched to new data by minimizing an energy term including both external forces from a thresholded data set and internal forces trying to maintain shape class and surface smoothness. Pfeifer et al. [8] segment both endocardium and epicardium, but the latter segmentation is obtained by identification of voxels surrounding the endocardium (within a maximum distance) by gray value. If this fails, a *global* mean atrial wall thickness of 5 mm is used. Recent studies show that LA wall thickness varies roughly between 0 and 7.7 mm [1], mostly smaller than the fall-back thickness used in [8]. Pfeifer et al. conclude that it is imperative to first segment the endocardium and to use that as a stepping stone for epicardium segmentation.

To our knowledge, accurate and automatic segmentation of LA *epicardium* has not yet been presented in literature.

3. METHODS

For endo- and epicardial segmentations, active contours are used with a feature function based on [6]. First the endocardial wall is segmented followed by the epicardial wall. Since reliable methods for endocardial segmentation already exist, our focus is on the epicardial segmentation.

3.1. Active contours

The position of the contour is represented parametrically by $\mathbf{v}(s) = (x(s), y(s))$, with x and y position coordinates of point s on the contour. The energy functional is written as

$$E^*_{contour} = \int_0^1 (E_{int}(\mathbf{v}(s)) + E_{ext}(\mathbf{v}(s)))\, ds, \quad (1)$$

where $E^*_{contour}$ is the total energy over the contour, E_{int} the internal and E_{ext} the external energy. The internal energy preserves contour smoothness by controlling elasticity and bending, expressed by first and second order derivatives respectively. By applying the Euler-Lagrange differential equation on the total energy over the contour a function is obtained, which can be interpreted as a force balance [7].

To find tissue transitions, a sampling grid of points

$$\mathbf{c}_{\lambda,\kappa} = (0, \lambda\varepsilon, \kappa\varepsilon), \;\; \lambda = -m, \ldots, m, \;\; \kappa = -l, \ldots, l \quad (2)$$

is chosen in a local coordinate system. This yields $(2l+1)$ equidistant points along the local contour normal. The sampling grid is $(2m+1)$ points wide, such that averaging over the $(2m+1)$ points (for every κ) helps suppressing noise influences along the contour tangential direction.

3.2. Endocardium

The blood pool-muscle transition is characterized by a large gradient. Therefore the gradient is a good feature to find the endocardial surface. A point $\tilde{\mathbf{c}}_\mathbf{i}$ within the sampling grid is chosen that maximizes the objective function.

$$\tilde{\mathbf{c}}_\mathbf{i} = \arg \max_{\mathbf{c}_{\lambda=0,\kappa}, \kappa=-l,\ldots,l} \{F(\mathbf{x_i} + \mathbf{M_i}\mathbf{c}_\kappa) - \delta||\mathbf{c}_\kappa||^2\}, \quad (3)$$

where $\mathbf{M_i}$ aligns the local coordinate system z-axis to the vertex normal $\mathbf{n_i}$, and δ balances feature strength and distance. Typically $l = 7$, $m = 0$ for the endocardium.

The feature function

$$F(\mathbf{x}) = \begin{cases} \sigma \mathbf{n_i} \nabla I(\mathbf{x}) \frac{g_m (g_m + ||\nabla I(\mathbf{x})||)}{g_m^2 + ||\nabla I(\mathbf{x})||^2} & I_- < I(\mathbf{x}) < I_+, \\ 0 & \text{otherwise} \end{cases} \quad (4)$$

projects the image gradient $\nabla I(\mathbf{x})$ onto the local contour normal $\mathbf{n_i}$ [6]. The fraction including g_m makes sure that points with image gradients higher than g_m do not give a higher response. Here, $\sigma = -1$, since we are looking for a gradient from light to dark. Finally, the feature function only applies to a specific intensity range (I_-, I_+).

3.3. Epicardium

For the epicardial wall, the endocardial contour is used to create a mask, showing only a 30 pixels wide band around the endocardial wall. Hysteresis thresholding is used [9], which involves two thresholds (t_h and t_l) and thus prevents the separation of isolated, mid-valued parts of the image. To find optimal thresholds, noise is assessed by convolving the data with a 5×5 neighbourhood operator yielding the mean gray value and standard deviation within the neighbourhood. Pixels at tissue transitions are discarded by fitting a curve to the standard deviation as a function of the mean gray value, and deleting values above the curve. Thus, only variation due to noise is obtained, for different tissues. The upper threshold t_h is set to t_{mf}, the muscle-fat transition value, resulting from a modified Otsu's threshold selection method [10] applied to the band histogram of a stack of neighbouring slices. The lower threshold is defined as $t_l = t_{mf} - \sigma_{mf}$, where σ_{mf} is obtained from the noise analysis. Based on its gray value (g) and the thresholds, each pixel is labeled. Outside the intensity range of -200 to 200 HU pixels are classified as C_o (e.g. blood pool or air). Otherwise pixels are labeled muscle C_m ($g > t_h$) or fat C_f ($g < t_l$). Gray values in between t_l and t_h are labeled C_m if a path to C_m pixels exists, otherwise C_f.

The epicardial contour is initialized with the final endocardial contour. The former can never be inside the latter. Since the gradient is not a reliable feature for the epicardial wall, the optimal epicardial position is defined by

$$\begin{aligned} \tilde{\mathbf{c}}_\mathbf{i} &= \mathbf{c}_\kappa, \text{ where} \quad (5) \\ \kappa &= \min(\{\kappa \mid \mu_{i\kappa} \in_h C_f\}) - 1, \\ \mu_{i\kappa} &= \sum_{\lambda=-m}^{m} \frac{I(\mathbf{x_i} + \mathbf{M_i}\mathbf{c}_{\lambda\kappa})}{2m+1}, \end{aligned}$$

with $\in_h$ meaning "element of, given the hysteresis rules". This means the minimal value minus one of κ is chosen for which the average gray value $\mu_{i\kappa}$ over λ is an element of the fat class. If no $\tilde{\mathbf{c}}_\mathbf{i}$ is found using Eq. 5, this will be found by interpolation using the two closest responsive neighbours of each side of such a vertex. Typically $l = 7$, $m = 1$ for the epicardium.

The external force for both endocardial en epicardial segmentation is defined by

$$F_{ext} = \text{Sign}(\mathbf{n_i} \cdot \mathbf{M_i}\tilde{\mathbf{c}}_\mathbf{i})\, \mathbf{n_i} \min\{\gamma, ||\tilde{\mathbf{c}}_\mathbf{i}||\}, \quad (6)$$

with γ the maximum desired step distance, to ensure a more controlled movement of the contour. After segmentation a wall thickness can be determined. The two curves are averaged with the use of corresponding points on both curves according to [11]. The average curve is obtained by iteration until it converges. The local distances can now be calculated by the L_2 norm of the difference vector between every pair of points on both curves, perpendicular to the average curve.

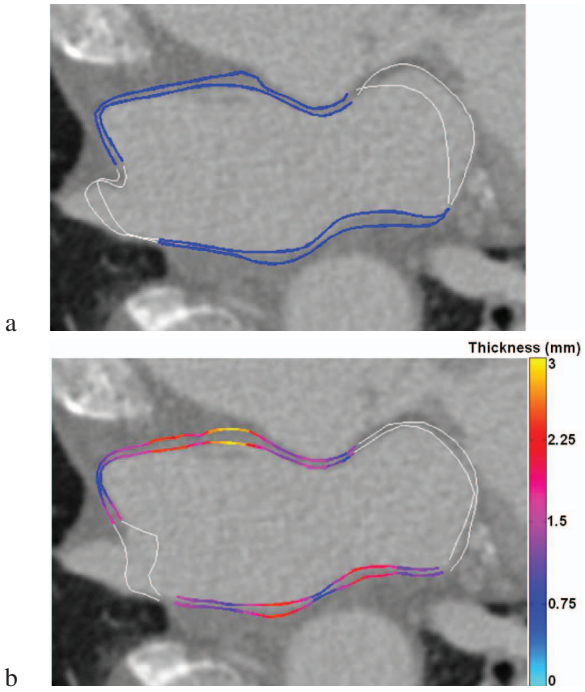

Fig. 1. (a) Manual segmentation (b) Automatic segmentation with colour coded thickness. White contour parts indicate the valve plane or PV ostium, these parts are discarded in the evaluation.

4. RESULTS

4.1. Data

Four clinical patient data sets were used. Contrast enhanced images were acquired by a Philips Brilliance 64 CT scanner (Philips Healthcare, Best, Netherlands) at 70% of the cardiac cycle, just before atrial contraction. All sets were helical CT scans of about 300 slices. Slice thickness was 0.67 mm, slice spacing was 0.33 mm. Images reconstructed were 512×512 pixels, with a resolution of about 0.30-0.40 mm per pixel. The images were acquired with a CT angiography (CTA) protocol and thus not specifically made for analyzing the left atrium.

4.2. Manual segmentation

Two experts, referred to as MP and RB, drew both endo- and epicardial contours consecutively on 29 slices by clicking a number of points. A spline was fitted through the selected points to obtain a smooth and closed contour. The experts were free to select window centre and window width of the viewer and the number of points to set.

4.3. Contour comparison

The endo- and epicardial walls of the selected slices were segmented using the proposed method, after manual initialisation. A damping force was introduced to reduce resonance in the last iterations. The method iterated one hundred times.

All were compared to manual segmentation using the distance measure. Two quantification methods were used, the root mean square (RMS), and the mean and standard deviation of the distances, per slice. Furthermore the mean wall thickness is compared between the different segmentations. Local wall thicknesses due to the manual and semi-automatic segmentations were measured at almost the same position.

On the differences, repeated measures analysis of variance (RMA) tests were performed. Thus, effects of experimental factors are assessed relative to the average response made by the subject on all conditions. RMA is only valid under 3 assumptions: normality, homogeneity of variance and sphericity. Non-sphericity was corrected for if necessary.

4.4. Segmentation and wall thickness results

The wall thicknesses found in the data set vary between about 0.5mm to almost 5.5mm, which corresponds to values found in literature [1, 12]. Figure 1 shows a manual segmentation and a typical segmentation result by the proposed method.

For comparison of the semi-automatic and manual segmentations, results from all slices were treated as if they came from one data set, and are presented in box plots (see Fig. 2). On the differences between *endocardial* segmentations (see Fig. 2a) a repeated measure analysis of variance (RMA) is applied. Both for the RMS ($p = 0.23$) and for the mean differences ($p = 0.27$) the results do not differ significantly from each other. The *epicardial* comparison with expert MP shows a slight underestimation by the proposed method, while the comparison with expert RB shows overestimation in all cases (see Fig. 2b). There is no significant difference between segmentations for the RMS values ($p = 0.18$), but there is significance for mean difference values ($p < 0.001$). The *wall thickness* comparison (see Fig. 2c) shows the same significant difference ($p < 0.001$) as for the epicardium comparison.

5. DISCUSSION & CONCLUSION

This paper presents the first semi-automatic LA wall thickness analysis method, based on CT images. The results of the algorithm are within inter expert variation. As expected, the the larger errors appear in the epicardial wall segmentation, since the transition is fuzzier than for the endocardium. Comments from one expert indicate he was not always sure while drawing the epicardial contour. This may have led to the difference among experts and with the automatic segmentations.

Some improvements may be suggested. Segmentation right next to, e.g., the orifices of the PVs may be hampered by missing edge information over large parts of the contours. An automatic detection of the pulmonary veins and the mitral valve may be incorporated, by inspection of the gradient perpendicular to the endocardial wall contour.

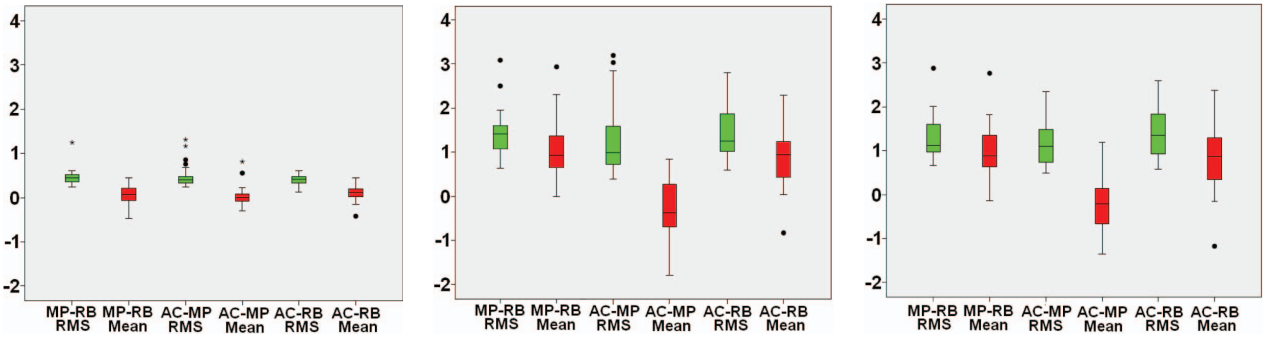

Fig. 2. Comparison between experts (MP-RB) and proposed method (AC-MP,AC-RB). RMS and mean difference (in mm) of the endocardium segmentation (a), epicardium segmentation (b), and wall thickness (c). Outliers are indicated with • and ∗.

For the epicardial wall detection, it would be interesting to inspect the regional histogram at different locations along the atrium wall instead of the global histogram. Thus, regional differences may be incorporated in the thresholding method.

It should be possible to attach a reliability measure to the results, based on the strength of the local feature(s).

The active contours method is performed for a fixed number of iterations. A stop criterion based on the *local* contour's energy may be incorporated. If the global energy is stable, it is still possible that some local deformations need to be done.

The extension from a 2D model to a 3D model is straight forward. This would not only improve the smoothness of the model, but would probably also increase the accuracy, since border information can be obtained in more directions.

In conclusion, left atrium endocardium and epicardium segmentation within the inter user variability range is achieved.

6. REFERENCES

[1] A E Becker, "Left atrial isthmus: anatomic aspects relevant for linear catheter ablation procedures in humans.," *J Cardiovasc Electrophysiol*, vol. 15, no. 7, pp. 809–812, 2004.

[2] K Lemola, M Sneider, B Desjardins, I Case, J Han, E Good, K Tamirisa, A Tsemo, A Chugh, F Bogun, Jr Pelosi F, E Kazerooni, F Morady, and H Oral, "Computed tomographic analysis of the anatomy of the left atrium and the esophagus: implications for left atrial catheter ablation," *Circulation*, vol. 110, no. 24, pp. 3655–3660, 2004.

[3] M John and N Rahn, "Automatic left atrium segmentation by cutting the blood pool at narrowings," in *MICCAI 2005*, JS Duncan and G Gerig, Eds. 2005, vol. 3750 of *Lect Notes Comput Sc*, pp. 798–805, Springer.

[4] R Karim, R Mohiaddin, and D Rueckert, "Left atrium segmentation for atrial fibrillation ablation," in *Proc SPIE: Medical Imaging 2008: Visualization, Image-guided Procedures, and Modeling*, Michael I. Miga and Kevin R. Cleary, Eds. 2008, vol. 6918, p. 69182U, SPIE.

[5] J Lötjönen, S Kivistö, J Koikkalainen, D Smutek, and K Lauerma, "Statistical shape model of atria, ventricles and epicardium from short- and long-axis mr images," *Med Image Anal*, vol. 8, no. 3, pp. 371–386, 2004.

[6] C Lorenz and J von Berg, "A comprehensive shape model of the heart," *Med Image Anal*, vol. 10, no. 4, pp. 657–670, 2006.

[7] C Xu and JL Prince, "Snakes, shapes, and gradient vector flow," *IEEE T Image Process*, vol. 7, no. 3, pp. 359–369, 1998.

[8] B Pfeifer, F Hanser, T Trieb, C Hintermüller, M Seger, G Fischer, R Modre, and B Tilg, "Combining active appearance models and morphological operators using a pipeline for automatic myocardium extraction," in *FIMH 2005*, AF Frangi, P Radeva, A Santos, and M Hernandez, Eds. 2005, vol. 3504 of *Lect Notes Comput Sc*, pp. 44–53, Springer.

[9] P L Rosin and T Ellis, "Image difference threshold strategies and shadow detection," in *Proc Brit Mach Vis Conf*. 1995, pp. 347–356, BMVA Press.

[10] P Liao, T Chen, and P Chung, "A fast algorithm for multilevel thresholding," *J Inf Sci Eng*, vol. 17, pp. 713–727, 2001.

[11] V Chalana and Y Kim, "A methodology for evaluation of boundary detection algorithms on medical images," *IEEE T Med Imaging*, vol. 16, no. 5, pp. 642–652, 1997.

[12] D Sanchez-Quintana, JA Cabrera, V Climent, J Farre, MC Mendonca, and SY Ho, "Anatomic relations between the esophagus and left atrium and relevance for ablation of atrial fibrillation," *Circulation*, vol. 112, no. 10, pp. 1400–1405, 2005.